# Three dimensional finite element study of crack in functionally graded material under thermal loading

**Parya Aghasafari[1*], Vahid Arabzadeh[1],Ali Daraei[1] ,Mahmoud Salimi[2]**

[1] Department of Mechanical Engineering, IUT University, 8415683111, Iran
[1] International Petro-Structure Co, 8015673611, Iran
[1] Department of Physics, UI University, 8174673441, Iran
[2] Faculty of mech.Eng dept, Institute of IUT, 8415683111, Iran
* Corresponding author: p.aghasafari@me.iut.ac.ir

## Abstract

This article focused on three-dimensional analyses of a functionally graded material plate which contains a semi-elliptical surface crack and subjected to transient thermal loading. Strain singularity around the crack front is simulated using collapsed 20 – node quarter – point brick elements. Three –dimensional displacement correlation technique is utilized to extract the mixed mode stress intensity factors around the crack front for different inclination angles of the semi-elliptic surface crack. Comparisons between current results and those from analytical and other numerical methods yield good agreement. Thus, it is concluded that the applied three-dimensional enriched finite elements are capable of accurately computing mixed-mode fracture parameters for cracks in FGMs.

**Keywords:** FGM, semi–elliptical inclined surface crack, displacement correlation technique, mixed modes stress intensity factors, finite element method

## 1. Introduction

Numerical simulations of crack initiation, propagation and branching are a computationally intensive process. Traditional finite element packages simulate the crack propagation problem either by using singularity elements or by using line spring elements with built-in fracture criteria. Recently, a popular method to do this task is the cohesive surface modeling of the fracture zone. Following the work of Baren blatt[2], Dugdale [3] ,and Willis [4], many researchers have addressed the issue to this approach. Nee-dleman[5] provided a framework for these parathion process starting from initial de-bonding in the cohesive zone. Larsson [6] used this approach to simulate crack growth in brittle materials, while Xia and Shih[7] simulated fracture inductile material sunder static loading. Camacho and Ortiz[8] have used cohesive surface modeling to study material fragmentation, while Xu and Needleman[9] used it to study dynamic crack tip in stabilities by allowing cracks to formal on element boundaries. The method by Xu and Needleman involves introducing special boundary elements between regular elements, where the boundary Elements obey a cohesive law. Three factors influence the cohesive law behavior, namely the cohesive Strength, the critical separation at cohesive strength and the fracture energy in the separation process. These Models obviate the need for a separate external fracture criterion in fracture simulations. The effects of Plasticity inside volumetric elements have been investigated using the embedded-process-zone cohesive Fracture model by Tvergaard and Hucthinson[10,11]. Gullerud and Dodds [12] have used 3-D cohesive Elements for modeling ductile crack growth. More recently Foulketal.[13] presented a procedure for Implementing the cohesive zone modeling a 3-D finite

element framework where zones of cracking are Known a-priori and cohesive zone elements are placed along these element boundaries.
Gao [14,15] proposed that materials undergoing brittle fracture have large non-linear elastic deformations and that a hyper elastic description of the crack tip behavior provides a better explanation of dynamic Crack tip in stabilities. Gao and Klein[16] developed a method, called the virtual internal bond(VIB)model ,In which a cohesive type law is directly incorporated in to the constitutive model. This is done by treating the Body as a collection of randomly distributed material points inter connected by a network of cohesive bonds.
The Cauchy–Bornrule of crystal elasticity is used to derive the overall constitutive relations. This is done by equating the strain energy of the bonds to the potential energy stored in the continuum due to applied loads and deformations. As this is implemented in a hyper elastic frame work deformation continuum mechanics, the Green–Lagrange strain tensor can be evaluated from deformation gradient, and the second Piola–Kirchoff stress tensor can be computed from the potential energy expression. The main advantage of this method is that, as in the cohesive boundary element approach [9], no separate fracture criterion is needed. Furthermore, the cohesive law is now embedded directly into the constitutive equations, thus no special boundary elements between regular elements are needed.
This study implements a finite element model to study the thermal fracture behavior of functionally graded materials. Stress intensity factors (SIF) are evaluated using a thermo mechanics and fracture mechanics approach. The results show that the components gradation of the FGM composites has significant influence on the specimens' thermal behavior.

## 2. Thermo-mechanical finite element modeling of FGM

A problem which is encountered in three-dimensional finite element analyses is the large number of elements and as a result, a remarkable and time consuming computation. Also, because of very rapid changes in the geometrical parameters around the crack front region, mesh generation of this region must be done with a great care. This may lead to increase the run time which makes it difficult to reach valid results and conclusion [17].
The main objective of this study is to model and analyze a three dimensional inclined semi-elliptic surface crack in a plate made of Functionally Graded Material (FGM). FGM is 100% zirconia-yttria (ZrO2-8wt%-Y2O3 ) at x=0 and 100% nickel-chromium–aluminum– zirconium (NiCrAlY) at x= t. The thermo mechanical properties of the FGM structure are assigned according to variation function by using the centroid of each finite element. This procedure is developed by utilizing ANSYS codes. A unique material property is assigned to each element with the help of this method.
In this study three different ratio regarding to modulus of elasticity (E) are considered as E2/E1= 20, E2/E1= 0.05 and homogeneous material case.E1and E2 are the values of the elastic module at x= 0 and x=t, respectively. Except elastic module a total of five material parameters are required to be known in order to carry out the transient thermal fracture analysis. These parameters are Poisson's ratio υ, thermal expansion coefficient αt, thermal conductivity k and density multiplied by specific heat ($\rho c_t$). ($\rho c_t$) can be evaluated using the relationship $D = {}^{k}/_{\rho c_t}$ where D is the thermal diffusivity.

$$E(x) = Ee^{\beta x} \quad 0 < x < t \qquad \textit{(Eq. 1)}$$
$$v(x) = ve^{\beta x} \quad 0 < x < t \qquad \text{(Eq. 2)}$$
$$\alpha(x) = \alpha e^{\beta x} \quad 0 < x < t \qquad \textit{(Eq. 3)}$$
$$k(x) = ke^{\beta x} \quad 0 < x < t \qquad \text{(Eq. 4)}$$
$$\rho c_t(x) = \rho c_t e^{\beta x} \quad 0 < x < t \qquad \text{(Eq. 5)}$$

$\beta$ is material constant and

$$\beta = {}^{1}/_{t}\, Ln\left({}^{E_2}/_{E_1}\right) \qquad \text{(Eq. 6)}$$

Table 1

Table 1

| Material | Modulus Of Elasticity (GPa) | Poisson's ratio | Coefficient of thermal expansion ($^{\circ}C^{-1}$) | Coefficient of thermal conductivity (W/mK) | thermal diffusivity ($m^2/s$) |
|---|---|---|---|---|---|
| Substrate (Ni) | 175.8 | 0.25 | $13.91\times10^{-6}$ | 7 | $2\times10^{-6}$ |
| Bond Coat (NiCrAIY) | 137.9 | 0.27 | $15.16\times10^{-6}$ | 25 | $8\times10^{-6}$ |
| Zirconia-Yttria | 27.6 | 0.25 | $13.91\times10^{-6}$ | 1 | $5\times10^{-6}$ |

In this paper combined thermal-structural analysis is studied. In the thermal analysis, first transient heat conduction in the FGM structure is conducted and consequently temperature distribution within the structure is computed. Afterwards, this temperature distribution is utilized as an input for the structural problem. While performing the analyses, it is assumed that the crack surfaces are completely insulated and the medium is free of any mechanical constraints. Furthermore, coupling of the thermal and structural problems are assumed to be through the calculated temperature distribution only since the inertia effects are not taken into account. During the solution, minimum and maximum time step sizes are entered. In order to overcome oscillations in the distribution of temperature, minimum time step size is taken to be very small and maximum time step size is chosen as not to be very large. By imposing temperature of the environment and applying free and forced convection coefficients on related surfaces of the FGM structure in time steps the problem is solved and calculated at each node. Then after computing the mixed mode stress intensity factors at the crack front nodes by utilizing the displacement correlation technique, the procedure of solving is repeated for each required time until the end time is reached.

## 3. The Displacement Correlation Technique (DCT)

Since the problem considered in this study is related to the inclined cracks (unsymmetrical), a complete crack model is needed to calculate the stress intensity factors. The figure below shows the full model which is to be used for mode I stress intensity factor calculation of an inclined crack.

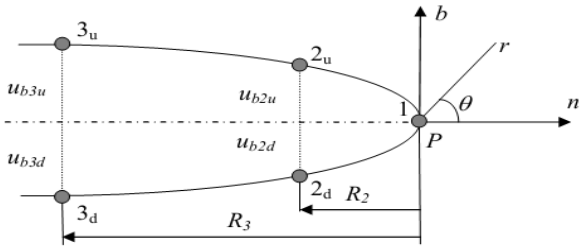


Fig 1- Deformed shape of the crack surface (non-symmetric)

The displacement component, which is required to calculate KI, at point P on the crack front can be expressed as

$$u_{\Delta}(r,\theta)=\left(\frac{1+\nu}{E}\right)\sqrt{\frac{2r}{\Pi}}\left\{k_{\imath}(s)\sin\left(\frac{\theta}{2}\right)\left[2(1-\nu)-\cos^2\left(\frac{\theta}{2}\right)\right]\right.$$

$$\left.-k_{\imath\imath}(S)\cos\left(\frac{\theta}{2}\right)\left[(1-2\nu)-\sin^2\left(\frac{\theta}{2}\right)\right]\right\} \qquad \text{(Eq. 1)}$$

$u_{\Delta}(r,\Pi)$is calculated by using equation (4.1). For the non-symmetric crack model, $u_{\Delta}(r,-\Pi)$ is also required. Thus, substituting $\theta=-\Pi$ into equation:

$$u_{\Delta}(r,-\Pi)=-\left(\tfrac{1+\nu}{E}\right)\sqrt{\tfrac{2r}{\Pi}}k_1 2(1-\nu) \qquad \text{(Eq. 2)}$$

Kı can be obtained as

$$k_1=\tfrac{\sqrt{2\Pi}\cdot E}{8(1-\nu^2)}\cdot\left[\lim_{r\to 0}\left\{\tfrac{u_{\Delta}(r,\Pi)-u_{\Delta}(r,-\Pi)}{\sqrt{r}}\right\}\right] \qquad \text{(Eq. 3)}$$

At the crach tip (i.e. $r\to 0$) , $\lim_{r\to 0}\left\{\frac{u_{\Delta}(r,\Pi)-u_{\Delta}(r,-\Pi)}{\sqrt{r}}\right\}=X$.Hence, equation

$$k_1=\tfrac{\sqrt{2\Pi}\cdot E}{8(1-\nu^2)}\cdot X \qquad \text{(Eq. 4)}$$

$$x=\frac{R_3^{3/2}(u_{\Delta\,2,0}-u_{\Delta\,2,3})-R_2^{3/2}(u_{\Delta\,3,0}-u_{\Delta\,3,3})}{\sqrt{R_2}\sqrt{R_3}(R_3-R_2)} \qquad \text{(Eq. 5)}$$

For r=$R_2$ → $\frac{u_{\Delta}(R_2,\Pi)-u_{\Delta}(R_2,-\Pi)}{\sqrt{R_2}}=\frac{u_{\Delta\,2,0}-u_{\Delta\,2,3}}{\sqrt{R_2}}=x+YR_2$

And

For r=$R_3$ → $\frac{u_{\Delta}(R_3,\Pi)-u_{\Delta}(R_3,-\Pi)}{\sqrt{R_3}}=\frac{u_{\Delta\,3,0}-u_{\Delta\,3,0}}{\sqrt{R_3}}=x+YR_3$

$$k_{\imath\imath}=\tfrac{\sqrt{2\Pi}\cdot E}{8(1-\nu^2)}\cdot\left[\lim_{r\to 0}\left\{\tfrac{u_0(r,\Pi)-u_0(r,-\Pi)}{\sqrt{r}}\right\}\right] \qquad \text{(Eq. 6)}$$

For r=$R_2$ → $\frac{u_0(R_2,\Pi)-u_0(R_2,-\Pi)}{\sqrt{R_2}}=\frac{u_{0\,2,0}-u_{0\,2,3}}{\sqrt{R_2}}=x+YR_2$

And

For r=$R_3$ → $\frac{u_0(R_3,\Pi)-u_0(R_3,-\Pi)}{\sqrt{R_3}}=\frac{u_{0\,3,0}-u_{0\,3,3}}{\sqrt{R_3}}=x+YR_3$

$$x = \frac{R_3^{3/2}(u_{0\,2,0}-u_{0\,2,3})-R_2^{3/2}(u_{0\,3,0}-u_{0\,3,3})}{\sqrt{R_2}\sqrt{R_3}(R_3-R_2)} \quad \text{(Eq. 7)}$$

$$k_{II} = \frac{\sqrt{2\Pi}\cdot E}{8(1-\nu^2)} \cdot X \quad \text{(Eq. 8)}$$

KIII can be calculated by the tangential displacement component at point P on the crack front. The tangential displacement component at this point is

$$u_c(r,\theta) = 2\left(\frac{1+\nu}{E}\right)\sqrt{\frac{2r}{\Pi}}k_m(s)\sin\left(\frac{\theta}{2}\right) \quad \text{(Eq. 9)}$$

For r=$R_2$ → $\frac{u_c(R_2,\Pi)-u_c(R_2,-\Pi)}{\sqrt{R_2}} = \frac{u_{c\,2,0}-u_{c\,2,3}}{\sqrt{R_2}} = x + YR_2$

And

For r=$R_3$ → $\frac{u_c(R_3,\Pi)-u_c(R_3,-\Pi)}{\sqrt{R_3}} = \frac{u_{c\,3,0}-u_{c\,3,3}}{\sqrt{R_3}} = x + YR_3$

$$x = \frac{R_3^{3/2}(u_{c\,2,0}-u_{c\,2,3})-R_2^{3/2}(u_{c\,3,0}-u_{c\,3,3})}{\sqrt{R_2}\sqrt{R_3}(R_3-R_2)} \quad \text{(Eq. 10)}$$

$$k_{III} = \frac{\sqrt{2\Pi}\cdot E}{8(1-\nu^2)} \cdot X \quad \text{(Eq. 11)}$$

$$\mu = \frac{E}{2(1+\nu)} \quad \text{(Eq. 12)}$$

Therefore, the total strain energy release rate under mixed mode loading is

$$G_T = G_1 + G_{II} + G_{III} = \frac{(1-\nu^2)}{E}\left\{k_1^2 + k_{II}^2 + \frac{k_{III}^2}{1-\nu}\right\} \quad \text{(Eq. 13)}$$

After the accuracy of the finite element model is checked out, the same model is used for the analyses of semi-elliptic inclined surface crack embedded in the FGM coating of composite structure. The finite element analyses of FGM coating- bond coat-substrate structure are carried out and the numerical results are calculated for various inclinations of three dimensional semi-elliptic surface crack, coating types, crack front angles and relative dimension of the crack with respect to FGM coating thickness.

## 4. Numerical results

There is a semi-elliptic inclined surface crack which has a length of 2c and a depth of a. The semi-elliptic crack has an inclination angle α, on the surface of the FGM at x=0. In the numerical analysis conducted, crack depth/ FGM thickness $^a/_t$ ratios and aspect ratio are used. These are as follows:

$$^a/_t = 0.2 \; and \; ^a/_c = {}^1/_2 \quad \text{(Eq. 14)}$$

In this analysis, the stress intensity factors are normalized by,

$$k_R = \sigma_0\sqrt{\frac{\Pi a}{Q}} \quad \text{(Eq. 15)}$$

Q is defined by,

$$Q = \begin{cases} 1 + 1.464(a/c)^{1.65} & \text{if } (\frac{a}{c}) \le 1 \\ 1 + 1 \cdot 464(c/a)^{1.65} & \text{if}(\frac{a}{c}) > 1 \end{cases} \quad \text{(Eq. 16)}$$

The schematic of the crack front can be seen at Figure 2. The validation of the model is done by modeling and analyzing the plate, which contains a semi-elliptic inclined surface crack, with finite dimensions subjected to uniform tension (figures 3 and 4). As it can be seen from these figures, the results of this study are plotted for $\alpha = 0$ *and* $\alpha = 30$. it can be said that the obtained results are in good agreement with that of Ayhan et al. [11]

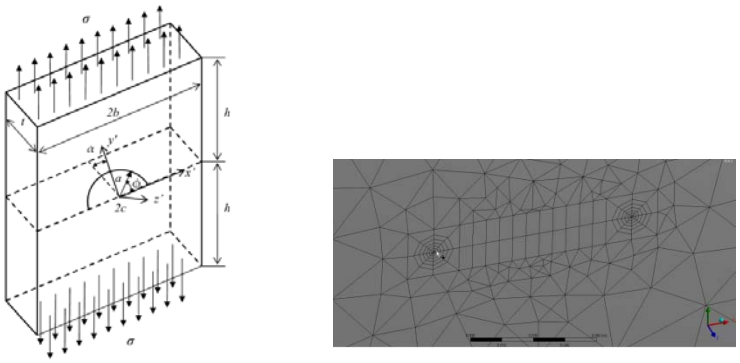

Fig 2- semi-elliptic inclined surface crack in a plate under uniform tensile remote stresses

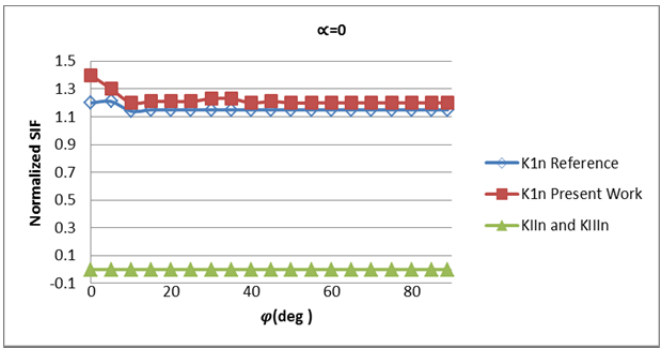


Fig 3- Comparisons of normalized mixed mode stress intensity factors for $0^o$ inclination angle

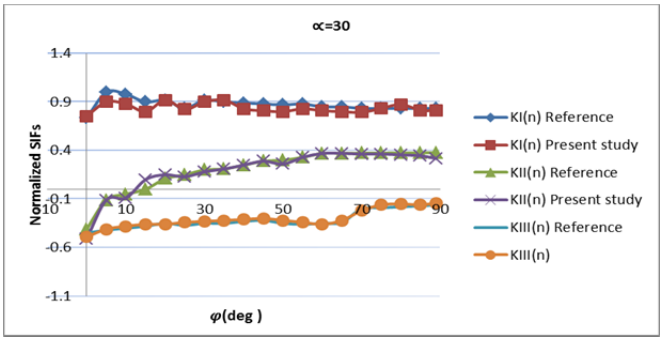


Fig 4- Comparisons of normalized mixed mode stress intensity factors for $30^o$ inclination angle

**Transient Thermal Loading**

The boundary conditions for this loading case are depicted in Figure 5.

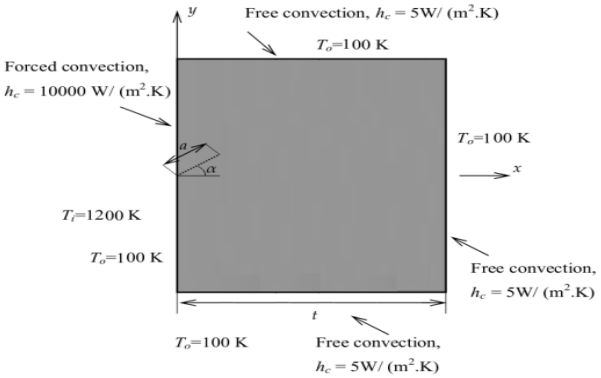


Fig 5- Thermal boundary conditions for the FGM coating, bond coat and substrate structure

It is assumed that the composite medium is initially stress-free at a high processing temperature of $T_i$ = 1200 K. Then, the other face of solid is left in an environment which has a temperature of $T_o$ = 100 K. The boundary conditions for this loading case are depicted in Figure 5. The thermo mechanical parameters used in the transient thermal analyses are described before. For the transient thermal analyses, inclination angles of $45^o$semi-elliptic surface crack are considered. It is seen that the normalized stress intensity factors rates go through a maximum in a short time period and then starts to decrease (Figures 6, 7 and 8) for different ratio of $E_2/E_1$. Figures 9 show the distribution of energy release around the crack front.

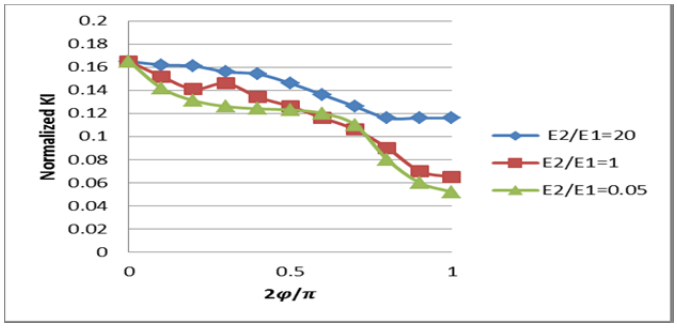


Fig 6- Distribution of normalized mode I stress intensity factors around crack front

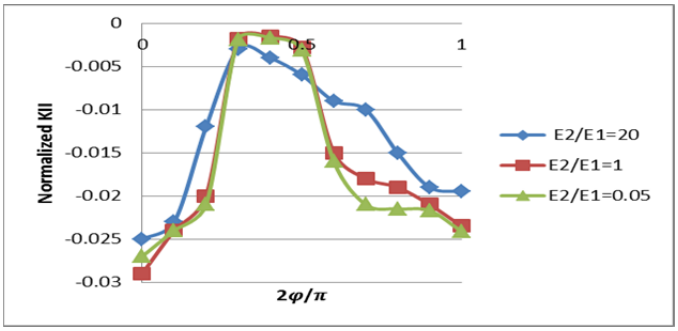


Fig 7- Distribution of normalized mode II stress intensity factors around crack front

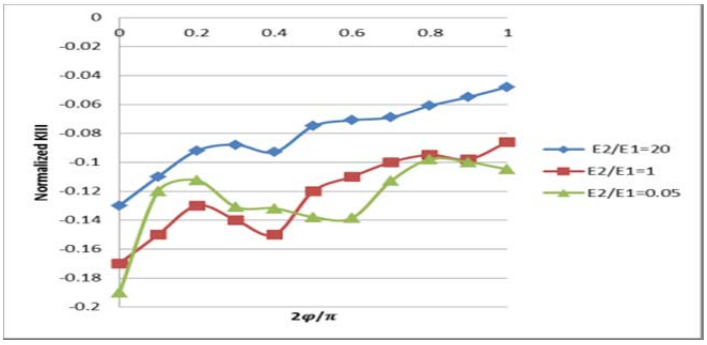


Fig 8- Distribution of normalized mode III stress intensity factors around crack front

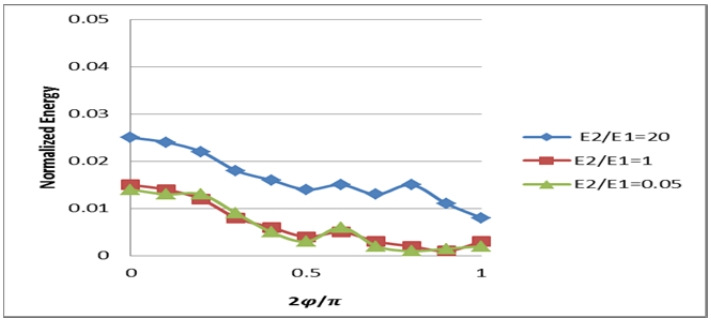


Fig 9- Distribution of normalized energy release rates around crack front

Figures 10 shows the distribution of temperature around the crack front at the time maximum values of normalized SIFs and energy release rates are reached.

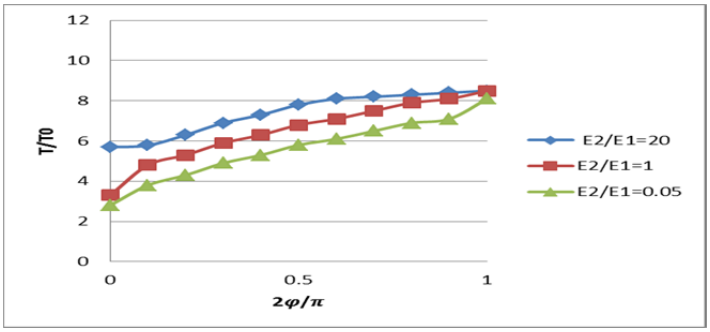


Fig 10- Distribution of temperature around crack front

In this study, an inclined semi-elliptical surface crack in an FGM structure is modeled in three dimension and fracture analyses are carried out by implementing finite element technique. For the model generations and finite element analyses, the multi-purpose finite element code ANSYS is used. The behavior of three dimensional inclined semi-elliptical surface cracks is examined under transient thermal loading for different ratios of material gradient. The mixed mode stress intensity factors and energy release rates around the crack front are calculated by utilizing displacement correlation technique.In order to verify the model and technique utilized in FGM structure, first of all, a plate and a semi-infinite solid with homogeneous material properties are modeled and analyzed under uniform tension. Then, the results obtained are compared to those given by Ayhan et al. [1 1]. It is observed that the figures generated for comparisons are in good agreement and therefore, it is concluded that this model can also be used for the finite element

analyses of the composite medium. The transient thermal analyses of the FGM structure are carried out for three different material gradients. It is assumed that the composite medium is initially at a high processing temperature. Then, this structure is left in an environment which is at a low temperature. Due to the high temperature difference, thermal stresses are induced at the composite structure containing an inclined semi-elliptical surface crack. Mixed mode SIFs and energy release rates are calculated along the crack front. It is observed that as the inclination angle increases, the normalized modes stress intensity factors decrease. The normalized energy release rates also decrease as the inclination angle increases. It is seen that for all inclination angles the normalized temperature increases as the crack front angle increases. It is could be concluded that material gradation has considerable effect on mode-II and mode-III stress intensity factors also. Thus, it is concluded that the 3D elements can be applied to calculate mixed-mode cracks in FGMs accurately and efficiently without needing special meshes near the crack front and detailed post-processing of the finite element solution.

**References**

[1] Andrews EW, Kim KS. Threshold conditions for dynamic fragmentation of ceramic particles. Mech Mater1998; 29:161–80.

[2] Barenblatt GI. The formation of equilibrium cracks during brittle fracture: general ideas and hypotheses, axially symmetric cracks. Appl Math Mech (PMM) 1959;23:622–36.

[3] Dugdale DS. Yielding of steel sheets containing slits . J Mech Phys Solids 1960;8:100–8.

[4] Willis JR . A comparison of the fracture criteria of Griffth and Barenblatt . J Mech Phys Solids 1967;15:151–62.

[5] Needleman A. A continuum model for void nucleation by inclusion debonding . J Appl Mech 1987;54:525–31.

[6] Larsson R.A generalized fictitious crack model based on plastic localization and discontinuous approximation. Int Journal Meth Eng.1995;38:3167–88.

[7] XiaL , Shih FC.Ductile crack growth—I. A numerical study using computational cells with micro structurally based length scales.J Mech Phys Solids 1995;43:233–59.

[8] Camacho GT, Ortiz M. Computational modeling of impact damage in brittle materials . Int J Solids Struct 1996;33:2899–938.

[9] Xu XP, Needleman A. Numerical simulation of fast crack growth in brittle solids. J Mech Phys Solids 1994;42(9):1397–434.

[10] Tvergaard V, Hutchinson JW. The relation between crack growth resistance and fracture process parameters in elastic–plastic solids. J Mech Phys Solids 1992;41:1377–97.

[11] Tvergaard V, Hutchinson JW. The influence of plasticity on mixed mode interface toughness. J Mech Phys Solids 1993;41:1119–35.

[12] Gullerud A, DoddsR.3-D modeling of ductile crack growth in thin sheet metals. Engng Fract Mech 1999;63:347–74.

[13] Foulk JW , Allen DH, HelmsKLE. Formulation of a three dimensional cohesive zone model for application to a finite element algorithm. Comput Meth Appl Mech Engng 2000;183:51–66.

[14] Gao H. A theory of local limiting speed in dynamic fracture . J Mech Phys Solids 1996;44:1453–74.

[15] Gao H. Elastic waves in a hyper elastic solid near its plane strain equibiaxial cohesive limit. PhilosMagLett1997;76:307–14.
[16] Gao H, Klein P. Numerical simulation of crack growth in an isotropic solid with randomized internal cohesive bonds .J Mech Phys Solids 1998;46:187–218.
[17] Wang QZ, Jia XM. More accurate stress intensity factor derived by finite element analysis for the ISMR suggested rock fracture toughness specimen-CCNBD. Int J Rock Mech Min Sci 2003;40:233e 41.